Thesis

A Study of Baseline Compensation System for Stable Operation of Gravitational-wave Telescope

Koseki Miyo

Department of Physics
University of Tokyo

MMM 2020

Abstract

a

要旨

2015 年、ブラックホール連星合体からの重力波 GW150914 を LIGO の 2 台の検出器が直接検出することに成功した。また 2017 年には Virgo を加えた 3 台の重力波検出器で連星中性子合体からの重力波 GW170817 を検出し、さらにフォローアップ観測によって電磁波対応天体も同定され、マルチメッセンジャー観測が確立された。そして 2020 年には KAGRA も LIGO と Virgo の重力波観測ネットワークに加わることで、より多くの重力波イベントの観測が期待される。

しかしながら、重力波は地球のどこでも検出できて視界に左右されないはずだが、現在稼働している干渉計型重力波検出器の DutyCycle は 60 % 程度である。これは悪天候時の高波や遠地でおきた地震などによる地面振動によって、干渉計の腕が変動し、干渉しなくなるためである。これら地面振動はおよそ 1 Hz 以下で数 10 km 以上のスケールで地面を揺らすが、現状の防振装置ではこのような低周波地面振動は防振できない。これは、グローバルな低周波の地面揺れを測定できるセンサーがないためである。

本論文では、基線長補償システムについて書かれている。このシステムは、レーザーひずみ計と呼ばれる地殻変動計測用の 1.5 km のレーザー干渉計をもちいて KAGRA の基線長伸縮をモニターし、その信号で、メインの KAGRA の干渉計が揺れないように防振をする。

この論文では、地面振動が干渉計に与える影響について調べられており、そしてその影響を低減するための基線長補償システムの原理と、その理論的性能、既存のシステムと比較した利点が調べられている。そして、このシステムを実際に KAGRA に組み込んだ性能評価実験が述べられている。この実験では、もっとも地面振動の影響を受けやすい 3 km の Fabry-Perot 光共振器に基線長補償システムを組み込み、この腕共振器の長さ変動を測定した。その結果、

Contents

Chapter 1

Background

In this chapter, we describe about gravitational-wave and detector.

1.1 Gravitational-wave

Gravtational-wave (GW) is a ripples of the space-time, which propagates at the speed of light. GW was predicted by A. Einstein in 1918, and is a result of the general theory of relativity. However because this strain is very small, the direct discovery of GWs have not done by LIGO until 2015.

1.1.1 Properties of GWs

Two polized transverse wave

The interval between two events in space-time is described with the metric tensor $g_{\mu\nu}$ as,

$$ds^2 = g_{\mu\nu}dx^\mu dx^\nu (\mu, \nu = 0, 1, 2, 3), \tag{1.1}$$

where dx^μ represents the coordinate distance of the events, and x^μ has 4 components; (ct, x, y, z).

In the general relativity theory[1], the metric tensor $g_{\mu\nu}$ is described by the

Einstein's equation;

$$R_{\mu\nu}\left(g_{\mu\nu}\right) - \frac{1}{2} g_{\mu\nu} R\left(g_{\mu\nu}\right) = \frac{8\pi G}{c^4} T_{\mu\nu}, \tag{1.2}$$

where $R_{\mu\nu}$ is the Ricci tensor, $R = g^{\mu\nu} R_{\mu\nu}$ is the Ricci scalar curvature, $T_{\mu\nu}$ is the energy-momentum tensor, G is the Newton's gravitational constan, and c is the speed of light.

GW is derived from this Einstein's equation when the metric can be described as the perturbation $h_{\mu\nu}$ to the Minkowsky space-time $\eta_{\mu\nu}$, thus

$$g_{\mu\nu} = \eta_{\mu\nu} + h_{\mu\nu}. \tag{1.3}$$

In this weak-field regime, the Einsteins's equation is reduced to a linearized wave-equation whose solution is represented as

$$h_{\mu\nu}(z,t) = \begin{pmatrix} 0 & 0 & 0 & 0 \\ 0 & -h_+ & h_\times & 0 \\ 0 & h_\times & h_+ & 0 \\ 0 & 0 & 0 & 0 \end{pmatrix} \cos\left[\omega\left(\mathrm{t} - \frac{\mathrm{Z}}{\mathrm{c}}\right)\right], \tag{1.4}$$

where ω is the angluar frequency of GW, z is the propagation direction of the wave, $h_+$and $h_\times$ are the independent polization of that. Therefore, GW is the transverse wave propagating with speed of light.

The two polization of GW are known as plus and cross polization, and these polization change the distance between two points as shown in Fig.1.1.

1.1.2 Sources of Gravitational-wave

Compact Binary Coalescence

Compact binary coalescence (CBCs), such as black holes and neutron stars, emit a characteristic chirp GW signal. The frequency of a hirp GW signal f_g increase as a function of time. This growing up is caused by loosing the angluar momentum of the system due to the emittion of GW.

Advanced LIGO have detected the first GWs from stellar-mass binary black holes (BBHs) in the first observation run (O1), which took place from September

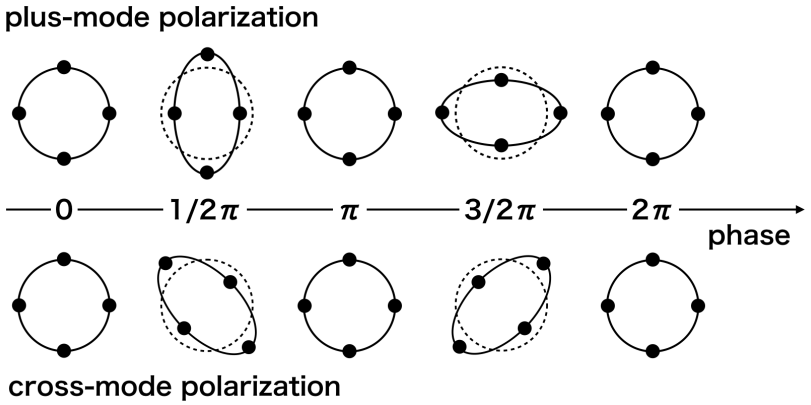

Figure 1.1: Polization of the GW propagating in the direction of the paper. These polization change the distance as the tidal motion.

12, 2015 until January 19, 2016. After this observation, Virgo detector joined the Advanced LIGO detectors and this network have detected the first detection of GWs from a binary neutron star inspiral in the second observation run (O2), which ran from November 30, 2016 to August 25, 2017. Moreover, observation of GWs from a total of seven BBHs [2].

Continuous GWs

Without rotating two objects, asymmetric spinning stars, such as neutron stars and pulsars, could produce detectable GWs which signal is also well defined [3, 4].

Burst GWs

In addition to continuous gravity waves, there are short suration GWs like a burst event. Supernovae are good candidates to emit te burst GWs [5]

Stochastic GWs

The stochastic background GWs are predicted[6, 7]. This background signal is originated from quantum fluctuations during inflation [8]. Basically, stochastic

bacground will appear like a random noise in an individual detector. However, it will be found like a coherent signal in two detector.

1.2 Interferometric Gravitational-wave detection

Basic design of a terrestrial GW detectors are Michelson interferometer [9]. This interferometer sensitives to the differential length change of its arms. This change is a strain caused by GWs. We assume that puls mode of GW is passing thorugh the interferometer perpendicularly.

1.2.1 Michelson Interferometer

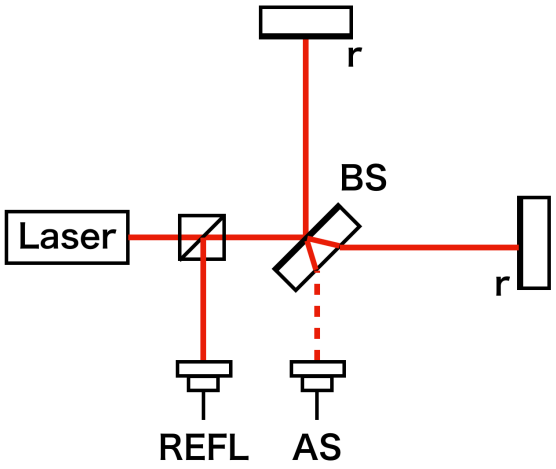

Figure 1.2: Michelson Interferometer.

Michelson interferometer is a converter from the optical phase difference of two lights to the amplitude modulation of a single light. Consider about the interferometer shown in Fig. 1.2. Incident light can be wrtten as,

$$E_{\text{in}} = E_0 e^{i\omega t}, \tag{1.5}$$

where E_0 is the amplitude and ω_0 is the angular frequency of the laser field . Two lights splited by the Beam Spliter (BS) interferer at the Anti-symetric (AS) port and Refrection (REFL) port. The output fieled at the AS port is represented as,

$$E_{\mathrm{AS}} = -\frac{1}{2} r E_0 e^{i(\omega_0 t - \phi_x)} + \frac{1}{2} r E_0 e^{i(\omega_0 t - \phi_y)}, \tag{1.6}$$

where r denote the amplitude reflectivity of the end mirrors, and ϕ_x and ϕ_x are the phase delay due to the light traveling in the x and y arms. This output signal can be represented as a single fieled as,

$$E_{\mathrm{AS}} = ir E_0 e^{i(\omega_0 t - (\phi_x + \phi_y)/2)} \sin\left(\frac{\phi_x - \phi_y}{2}\right). \tag{1.7}$$

Wwe find that the amplitude of the output light is a function of the difference between two phases; $\phi_x - \phi_y$. Furthermore, the power of output light at the AS port is obtained by squaring the Eq.1.7,

$$P_{\mathrm{AS}} \quad = \left[r \sin(\phi_-)\right]^2 P_0 \tag{1.8}$$

Similarly, power of the output light as REFL port is written as,

$$P_{\mathrm{REFL}} \quad = \left[(r \cos(\phi_-))\right]^2 P_0. \tag{1.9}$$

Therefore, we can measure the optical phase difference as the amplitude changes using a Photo Detector (PD) and detect GWs.

1.2.2 Static Response

Consider the error of the interferometric strain measurement. Bacause the optical phase ϕ_- is given by

$$\phi_- = \frac{4\pi L_-}{\lambda}, \tag{1.10}$$

where L_- is the differential length changes of its arms and λ is the wavelength of the input laser, the strain h is represented as

$$h = \frac{\Delta L_-}{L} = \frac{\lambda}{4\pi L} \Delta\phi_- + \frac{L_-}{L}\left(\frac{\Delta f}{f}\right). \tag{1.11}$$

Moreover, according to Eq.(1.8), because infinitesimal change of the optical phase $\Delta\phi_-$ is given by

$$\Delta\phi_- = \frac{\tan(\phi_-)}{2}\left[\left(\frac{\Delta P_{\rm AS}}{P_{\rm AS}}\right) + \left(\frac{\Delta P_0}{P_0}\right)\right], \tag{1.12}$$

where ΔP_0 is the fluctuation of the input laser and $\Delta P_{\rm AS}$ is a power fluctuation at AS port, finaly, we get a strain as a function of several fluctuation of parameters below;

$$h = \frac{\lambda}{8\pi L}\tan(\phi_-)\left[\left(\frac{\Delta P_{\rm AS}}{P_{\rm AS}}\right) + \left(\frac{\Delta P_0}{P_0}\right)\right] + \frac{L_-}{L}\left(\frac{\Delta f}{f}\right). \tag{1.13}$$

According to Eq.(1.13), in order to increase the interferometric strain measurement, we should do below;

- we should expand the baseline length L.
- we should operate the Michelson intereferometer at dark fringe, which means $\phi_- \to 0$, in order to decrease the noise contribution from $(\Delta P_{\rm AS}/P_{\rm AS})$ and $\Delta P_0/P_0$ to the strain h.
- we should use asymmetric arm so that $L_0 \to 0$, in order to decrease the noise contribution from the laser frequency fluctuation $\Delta f f$

1.3 Enhancement of the sensitivity

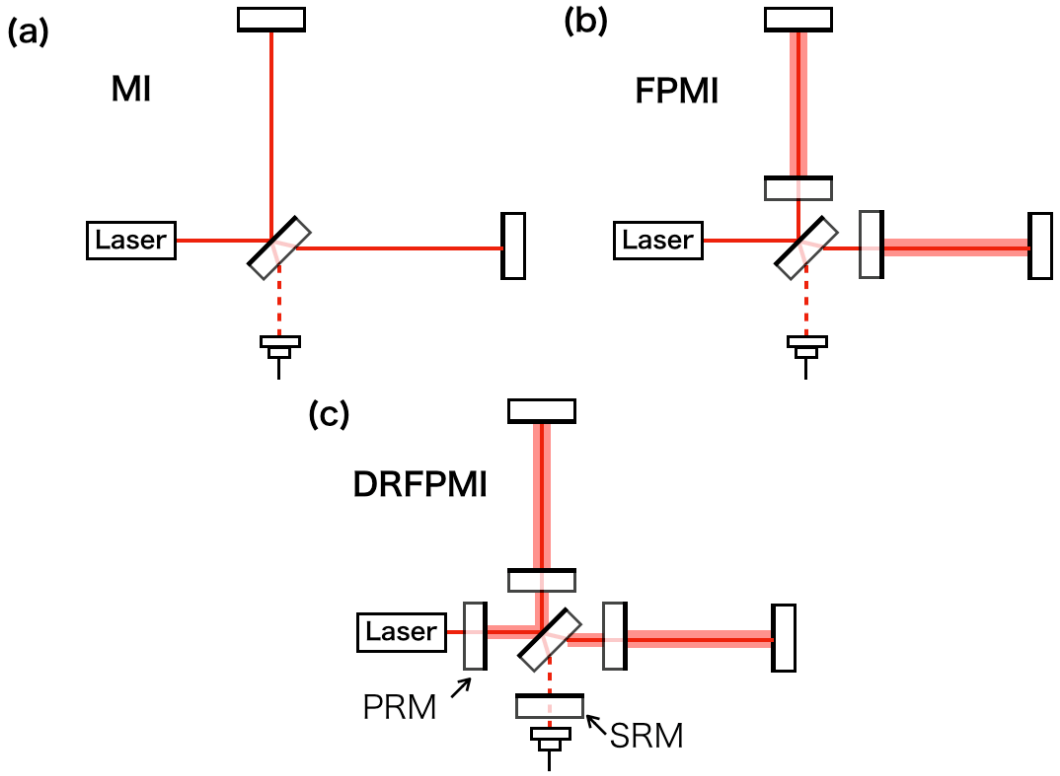

Figure 1.3: Configuration of interferometric GW detector. (a) Michelson interferometer (MI) (b) Michelson interferometer with two Fabry-Perot optical cavities (FPMI). (c) Dual-Recycled FPMI (DRFPMI)

In order increase the sensitivity, current interferometric GW detector use the Dual-Recycled Fabry-Perot Michelson Interferometer (DRFPMI).

1.3.1 Fabry-Perot Michelson Interferometer (FPMI)

Fabry-Perot Optical Cavity

Fabry-Perot optical cavity increase the effective baseline linegth. Consider the Fabry-Perot optical cavity composed of two mirrors separated by L as shown in

Fig.1.4a. In this figure, $E_{\rm in}$, $E_{\rm r}$, $E_{\rm t}$, E are the incident, reflected, and transmitted fields respectively, r_j and t_j are the amplitude reflectivity and transsivity of j-th mirrors ($j = 1, 2$). The averaged bounce number in a Fabry-Perot cavity $\mathcal{N}_{\rm FP}$ is written as [10]

$$\mathcal{N}_{\rm FP} = \frac{2\mathcal{F}}{\pi}, \tag{1.14}$$

where $\mathcal{F}$ is a finesse given as

$$\mathcal{F} = \frac{\pi\sqrt{r_1 r_2}}{1 - r_1 r_2}. \tag{1.15}$$

However, in order to resonate the optical cavity, the displacement of the cavity length within linewidth calculated as the width at half maximum (FWHM)

$$L_{\rm FWHM} = \frac{\lambda}{2\mathcal{F}}. \tag{1.16}$$

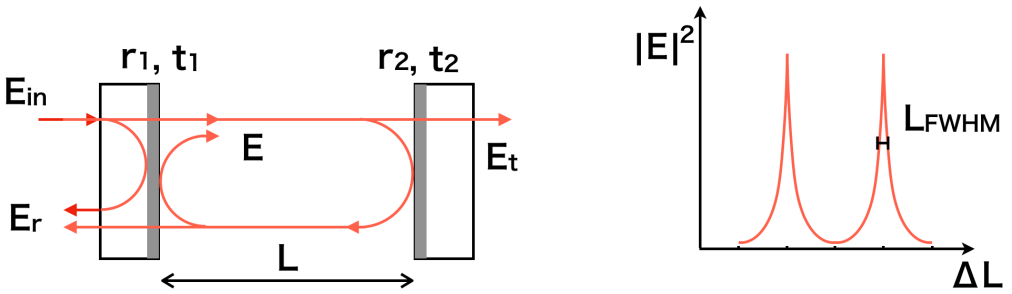

(a) Fabry-Perot optical cavity composed of two mirrors separated by L.

(b) Intra-cavity power as a function of displacement of cavity length.

Figure 1.4: Fabry-Perot optical cavity.

1.3.2 Dual-Recycled FPMI (DRFPMI)

As shown in Fig.1.3(c), final configuration of the current GW is DRFPMI which has two recycling optical cavity [11].

Power Recycle

In order to decrease shot noise, power recycling technique is used. In this technique, additional mirror is installed between laser and interferometer to increase the effective laser power by recycling the reflected light from the interferometer. Increaseing the laser power, the noise to signal ratio of shot noise is decrease as mentioned later.

Signal Recycle

Signal recycling mirror, which is installed on the AS port, is for tunning the frequency band. This mirror enhance the GW signal by recycling the output signal from the interferometer.

1.3.3 Noise

In terms of the interferometric GW detector, noise can be classified into two noises; detection noise and displacement noise of the testmass.

Shot Noise

In an ideal case that the test mass is not disturbed and as the free mass, the noise of the interferometer is limited by the shot noise.

Shot noise is a noise associated with the fluctuation of the number of photons at the photo detector. In case that the number of photons N are large enough ($N \gg 1$), the number of photon obey the Gaussian distribution with standard deviation of $\sqrt{N}$. Therefore, if laser power P incidents in the detector, shot noise has a relation with the power;

$$P_{\rm shot} \propto \sqrt{P} \quad [W/\sqrt{\rm Hz}]. \tag{1.17}$$

One can find that shot noise is a white noise, which propotional to the square-root of the incident power.

Here, according to Eq.(1.8), relative error of power at the detector is given by

$$\frac{\Delta P_{\rm AS}}{P_{\rm AS}} \propto \frac{1}{\sqrt{P_0}} \quad [1/\sqrt{\rm Hz}], \tag{1.18}$$

where $P_{\rm AS}$, $\Delta P_{\rm AS}$ are the power at the photo detector, P_0 is the power of the incident beam. This shows that we increasing the input power can decrease the shot noise.

Seismic Noise

Seismic noise is the largest displacement noise for interferometric GW detector. Seismic waves from various excitation sources disturbe the test mass through the mechanical structures. Therefore, in order to reduce the seismic noise, it is necessary to suspend the test masses far from the excitation sources. More details are described in the next chapter.

Newtonian Noise

Unlike the seismic noise mentioned above, the Newtonian noise is a noise that the density fluctuation of surrounding objects disturbes the test mass by gravitational interaction. Because this noise propagate through space, it can not isolate by using the vibration isolation scheme. Although the noise does not affects on the current 2nd generation GW detectors, it will contamintate on the next 3rd generation detectors.

In order to reduce the Newtonian noise, the feedforward control using the seismometer array is proposed.

Thermal Noise

In addition to external disturbances such as the seismic origin noise, the mirror substrate and surface particles cause random thermal motion generate displacement noise. This thermal noise can be classified into two; 1) mirror thermal noise 2) mirror coating thermal noise [12].

The displacement noise of the mirror thermal noise of the mirror with temperature T is given by [13, 14]

$$G_{\rm SB}(f) = \frac{4k_BT}{\omega}\frac{1-\sigma^2}{\sqrt{\pi}Ew_0}\phi_{\rm sub}(f), \tag{1.19}$$

where k_B is a Boltzmann constant, ω is angular frequency, σ, E, $\phi_{\rm sub}$ are a Poisson's ratio, Young's modulus, and mechanical loss angle of the bulk of the mirror respectively, and ω_0 is a beam radius. One can find that the mirror thermal noise is decreased by lower temperature or increase the beam radius.

The displacement noise of coating thermal noise is given by [14, 15]

$$G_{\rm CB}(f) = G_{\rm SB}(f)\left(1 + \frac{2}{\sqrt{\pi}}\frac{1-2\sigma}{1-\sigma}\frac{\phi_{\rm coat}}{\phi_{\rm sub}}\frac{d}{w_0}\right), \tag{1.20}$$

were d,$\phi_{\rm coat}$ are depth and loss angle of the coating.

1.4 Large-scale Terrestrial Laser Interferometers

Large-scale baseline is a essential feature of interferometric GW detectors for improving the sensitivity.

1.4.1 Terrestrial Laser Interferometers

So far, various interferometric GW detectors are developed in many places. These detectors are listed table 1.1.

Table 1.1: Terrestrial laser interferometers [16, 17]

Generation	Project	Baseline [m]	Bedrock
1st	LISM	10	Granite/gneiss
	CLIO	100	Granite/gneiss
	TAMA	300	Sedimentary soil [18]
	GEO	600	Sedimentary rock
2nd	aLIGO L1	4000	Sedimentary soil
	aLIGO H1	4000	Sedimentary rock
	aVirgo	3000	Sedimentary rock
	KAGRA	3000	Granite/gneiss
3rd	ET	10000	Granite/gneiss (Planning)

1st Generation

The first generation GW detectors (LISM [19], CLIO [20], TAMA [21], GEO [22]) are small-scale detectors and for test-bench of next generation detectors.

2nd Generation

The second generation GW detectors (KAGRA[23], Advanced Virgo[24], Advanced LIGO[25]) are first large-scale detectors for the enough sensitivity to detect GW signal.

3rd Generation

The third generation GW detector (now ET is proposed) has a few km-scale detectors.

1.4.2 Degradation of duty cycle

Large-scale baseline makes it difficult to keep the long arm cavity at the resonant state because low-frequency seismic noise disturbs the baseline length.

In case the short-scale baseline, the low-frequency seismic noise did not disturb the baseline length because the motion move the arm cavity as a singl object. However, in case the long-scale baseline, the seismic motion below 1 Hz move the two mirrors of the arm cavity with no correlation. Especially around 0.2 Hz, amplitude of microseisms caused by ocean activities are larger than the linewidth of arm cavity. This means that the duty cycle of interferometric GW detectors are limited by these low-frequencies.

1.4.3 Improvement of duty cycle

Low-frequency seismic noise potentilally cause the lock acquisition failure or lock loss.

Arm length stabilization (ALS)

ALS is a technique to reduce the RMS of arm cavity length using frequency-doubled auxiliary lasers before locking the cavity using main laser [26, 27]. The wavelength of this auxliliary laser is half of the main infrared laser (1064 nm), thus linewidth is also half according to Eq.(1.16). This means that the auxiliary laser is more easy to lock the arm cavity than the main laser. Therefore, onece locking the arm cavity using auxiliary laser, ALS system can reduce the RMS of arm cavity length fluctuation using the feedback signal of the auxiliary system so that the main laser can lock the arm caivty. Owing to this system, lock aquisition takes less than 10 minutes.

Early earthquake alert

Although ALS system can bring the interferometer to the observation state in a sufficiently short time, this is used in only the lock aquisition phase not observation phase due to the control noise. In the obseravtion phase, we can only use the main laser with narrow linewidth as a sensor for measurering the baseline length. Moreover, we have to use a narrow dynamic range and weak actuator not to contaminate the GW sensitivity with the actuator noise. In this situation, if disturbance will excess the range of sensors and actuators, the cavity can not keep the locking state.

Actually, duty cycle of GW detectors are limited by the low-frequency seismic noise in which the vibration isolation system could not attenuate the motion. Especially long period earthquake limites the duty cycle [28].

1.5 Outline of thesis

本論文では、長期線化によって引き起こされる DutyCycle の低下についての考察と、それを解決する防振システムの開発が述べられている。

1.6 Summary of the Chapter

Bibliography

[1] Albert Einstein. The Foundation of the General Theory of Relativity. *Annalen Phys.*, 49(7):769–822, 1916. [Annalen Phys.354,no.7,769(1916)].

[2] BP Abbott, R Abbott, TD Abbott, S Abraham, F Acernese, K Ackley, C Adams, RX Adhikari, VB Adya, C Affeldt, et al. Gwtc-1: a gravitational-wave transient catalog of compact binary mergers observed by ligo and virgo during the first and second observing runs. *Physical Review X*, 9(3):031040, 2019.

[3] Paola Leaci, LIGO Scientific Collaboration, Virgo Collaboration, et al. Searching for continuous gravitational wave signals using ligo and virgo detectors. In *Journal of Physics: Conference Series*, volume 354, page 012010. IOP Publishing, 2012.

[4] Mark Hereld. A search for gravitational radiation from psr 1937+ 214. 1984.

[5] Christian D Ott, Adam Burrows, Eli Livne, and Rolf Walder. Gravitational waves from axisymmetric, rotating stellar core collapse. *The Astrophysical Journal*, 600(2):834, 2004.

[6] AA Starobinskii. Spectrum of relict gravitational radiation and the early state of the universe. *JETP Letters*, 30:682–685, 1979.

[7] Nelson Christensen. Stochastic gravitational wave backgrounds. *Reports on Progress in Physics*, 82(1):016903, nov 2018.

[8] Alan H. Guth. Inflationary universe: A possible solution to the horizon and flatness problems. *Phys. Rev. D*, 23:347–356, Jan 1981.

[9] Rainer Weiss. Electronically coupled broadband gravitational antenna. 1972.

[10] Masaki Ando. *Power recycling for an interferometric gravitational wave detector*. PhD thesis.

[11] Brian J Meers. Recycling in laser-interferometric gravitational-wave detectors. *Physical Review D*, 38(8):2317, 1988.

[12] Dan Chen. *Study of a cryogenic suspension system for the gravitational wave telescope KAGRA*. PhD thesis, University of Tokyo, 2016.

[13] Yu. Levin. Internal thermal noise in the ligo test masses: A direct approach. *Phys. Rev. D*, 57:659–663, Jan 1998.

[14] Kenji Numata, Masaki Ando, Kazuhiro Yamamoto, Shigemi Otsuka, and Kimio Tsubono. Wide-band direct measurement of thermal fluctuations in an interferometer. *Phys. Rev. Lett.*, 91:260602, Dec 2003.

[15] Gregory M Harry, Andri M Gretarsson, Peter R Saulson, Scott E Kittelberger, Steven D Penn, William J Startin, Sheila Rowan, Martin M Fejer, DRM Crooks, Gianpietro Cagnoli, et al. Thermal noise in interferometric gravitational wave detectors due to dielectric optical coatings. *Classical and Quantum Gravity*, 19(5):897, 2002.

[16] Chiang-Mei Chen, James M Nester, and Wei-Tou Ni. A brief history of gravitational wave research. *Chinese Journal of Physics*, 55(1):142–169, 2017.

[17] Mark G. Beker. *Low-frequency sensitivity of next generation gravitational wave detectors*. PhD thesis, Vrije U., Amsterdam, 2013.

[18] 新藤 静夫. 武蔵野台地の地下地質. **地學雑誌**, 78(7):449–470, 1970.

[19] Shuichi Sato, Shinji Miyoki, Souichi Telada, Daisuke Tatsumi, Akito Araya, Masatake Ohashi, Yoji Totsuka, Mitsuhiro Fukushima, Masa-Katsu Fujimoto, LISM Collaboration, et al. Ultrastable performance of an underground-based laser interferometer observatory for gravitational waves. *Physical Review D*, 69(10):102005, 2004.

[20] M Ohashi, K Kuroda, S Miyoki, T Uchiyama, K Yamamoto, K Kasahara, T Shintomi, A Yamamoto, T Haruyama, Y Saito, et al. Design and construction status of clio. *Classical and Quantum Gravity*, 20(17):S599, 2003.

[21] Masaki Ando, Koji Arai, Ryutaro Takahashi, Gerhard Heinzel, Seiji Kawamura, Daisuke Tatsumi, Nobuyuki Kanda, Hideyuki Tagoshi, Akito Araya, Hideki Asada, et al. Stable operation of a 300-m laser interferometer with sufficient sensitivity to detect gravitational-wave events within our galaxy. *Physical Review Letters*, 86(18):3950, 2001.

[22] Hartmut Grote, LIGO Scientific Collaboration, et al. The geo 600 status. *Classical and Quantum Gravity*, 27(8):084003, 2010.

[23] Ando M. Arai K. et al. Akutsu, T. Kagra: 2.5 generation interferometric gravitational wave detector.

[24] F Acernese, M Agathos, K Agatsuma, D Aisa, N Allemandou, A Allocca, J Amarni, P Astone, G Balestri, G Ballardin, et al. Advanced virgo: a second-generation interferometric gravitational wave detector. *Classical and Quantum Gravity*, 32(2):024001, 2014.

[25] Junaid Aasi, BP Abbott, Richard Abbott, Thomas Abbott, MR Abernathy, Kendall Ackley, Carl Adams, Thomas Adams, Paolo Addesso, RX Adhikari, et al. Advanced ligo. *Classical and quantum gravity*, 32(7):074001, 2015.

[26] Adam J Mullavey, Bram JJ Slagmolen, John Miller, Matthew Evans, Peter Fritschel, Daniel Sigg, Sam J Waldman, Daniel A Shaddock, and David E McClelland. Arm-length stabilisation for interferometric gravitational-wave detectors using frequency-doubled auxiliary lasers. *Optics express*, 20(1):81–89, 2012.

[27] Kiwamu Izumi. *Multi-Color Interferometry for Lock Acquisition of Laser Interferometric Gravitational-wave Detectors*. PhD thesis, University of Tokyo, 2012.

[28] S Biscans, J Warner, R Mittleman, C Buchanan, M Coughlin, M Evans, H Gabbard, J Harms, B Lantz, N Mukund, A Pele, C Pezerat, P Picart, H Radkins, and T Shaffer. Control strategy to limit duty cycle impact of earthquakes on the LIGO gravitational-wave detectors. *Classical and Quantum Gravity*, 35(5):055004, jan 2018.